

Shape changes of spheroidal and rectangular grains driven by excess free energy

Hidehiko Tanaka*

Advanced Materials Laboratory, National Institute for Materials Science, 1-1 Namiki, Tsukuba-shi, Ibaraki, 305-0044 Japan

Received 1 July 2003; received in revised form 2 September 2003; accepted 13 September 2003

Abstract

Shape changes occurring in spheroidal and rectangular solid grains were theoretically investigated on the basis of the free energy theory for material transport. It was assumed that material transport in a non-equilibrium system was driven by excess free energy so that the system becomes an equilibrium state. The rate equation for material transport of solid in a non-equilibrium state was derived from this assumption. Using the equation, rates of shape changes for spheroidal and rectangular grains were formulated. From the rate equations, shape changes toward equilibrium shapes were simulated. It was found that elongated grains change their shapes more rapidly than nearly round and cubic grains.

© 2003 Elsevier Ltd. All rights reserved.

Keywords: Diffusion; Grain size; Surface; Theory

1. Introduction

Very fine ceramic powders are important raw materials in industry.^{1,2} They are sintered at high temperature, and are supplied as many suitable industrial parts. The grains in these powders usually have irregular shapes. If such grains are heat-treated at high temperature, and are extremely fine, they will change their shape toward an equilibrium shape. When the grain is isotropic, it will become a sphere, and when the grain is of a cubic crystallographic system, it will become a cube. During the shape changes, the free energy associated with surface area decreases until the grains become a sphere or a cube. Grains with irregular shapes have more surface energy than an equilibrium state. It is thus considered that the excess free energy stored on the grain surface is the driving force for material transport for shape change.

The same phenomenon happens in sintering and grain growth of metal and ceramic powders. When powder is sintered at high temperature, grains join together, losing surface area and creating a grain boundary.^{3–5} During this process, the sum of surface energy and grain

boundary energy in the powder must decrease. This means that the powder has excess free energy and that sintering and grain growth proceed in the direction that total free energy decreases. When polycrystalline material is heated at high temperature, grain growth will take place. Grains larger than the average size grow and the smaller grains shrink.^{3,6} The total grain boundary energy in a polycrystalline solid must decrease. It seems that the total grain boundary energy drives grain growth in polycrystalline material.

From these phenomena, we can consider that the driving force for material transport in sintering and grain growth is excess free energy associated with the surface and grain boundary. The author and Y. Inomata have been investigating sintering and grain growth from the viewpoint of the free energy theory.^{7–13} The theory assumed that the excess free energy stored in a system directly activates material transport, changing a system toward an equilibrium state, and a rate equation for material transport was proposed. From this theory, sintering and grain growth have been successfully analyzed.

The purpose of this work is to apply this theory to the simple case of shape change of small elongated grains. In this paper, first we discuss derivation of the rate equation for diffusion material transport from the free energy theory. Second we apply the rate equation to

* Tel.: +81-298604476; fax: +81-298513613.

E-mail address: tanaka.hidehiko@nims.go.jp (H. Tanaka).

shape changes of spheroidal and rectangular solid grains, and formulate rate equations for their shape changes. The shape changes are simulated and discussed from numerical calculations with the rate equations.

2. Free energy theory for material transport

If a system is in a non-equilibrium state, it has excess free energy ΔG over an equilibrium state, so some rate process will take place, and ΔG will decrease toward 0. In order to analyze this process, Inomata assumed that the rate must be in proportion to ΔG and a frequency of atom jump, and proposed the following equation.¹³

$$u = v_0 \exp\left(-\frac{\Delta G_m^*}{RT}\right) \psi \left\{1 - \exp\left(-\frac{\Delta G}{RT}\right)\right\}, \quad (1)$$

where u is the rate of the process, v_0 is the vibration frequency of atom, ΔG_m^* is the activation energy for atom jump or migration, and R and T are the gas constant and temperature, respectively. ψ is the measure unit for the rate process, which is volume or mass in the case of solid diffusion.

We consider here volume diffusion of solids. Fig. 1 shows a volume V with surface S , where dv is flowing from a small volume dV with cross sectional area $a(x)$ along diffusion path $\lambda_x(x)$ to outlet a_{out} . $a_m(x)$ is the mean cross sectional area of diffusion from $a(x)$ to a_{out} , and ΔG is excess free energy stored in the volume V . ψ in Eq. (1) is then volume diffusing from V . ψ is in proportion to the volume l_0^3 carried by one atom jumping. ψ is also in proportion to cross sectional area, which is expressed as a_x/l_0^2 in a non-dimensional unit, where a_x is effective diffusion area. ψ is in inverse proportion to diffusion length λ_x/l_0 , where λ_x is effective diffusion length. Substituting $\psi = \gamma(l_0^3)(a_x/l_0^2)/(\lambda_x/l_0)$ in

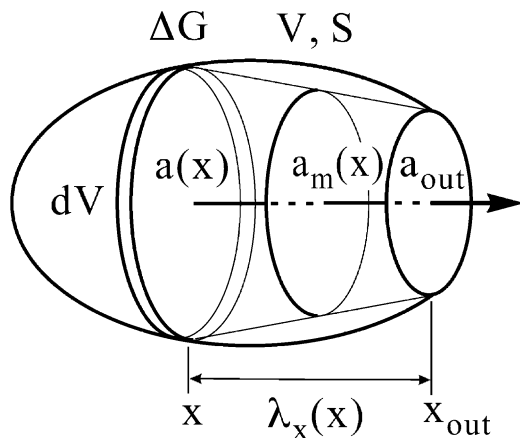


Fig. 1. Schematic showing diffusion material transport activated by excess free energy. Volume dv flows from a small volume dV with cross-sectional area $a(x)$ through mean cross-sectional area $a_m(x)$ along length λ_x to outlet a_{out} . ΔG is excess free energy in a system having volume V and surface S .

to Eq. (1), the material transport rate by diffusion dv/dt is written by Eq. (2).

$$\frac{dv}{dt} = \gamma l_0^2 v_0 \exp\left(-\frac{\Delta G_m^*}{RT}\right) \left(\frac{a_x}{\lambda_x}\right) \left\{1 - \exp\left(-\frac{\Delta G}{RT}\right)\right\}, \quad (2)$$

where γ is a constant depending on the crystal structure of the solid and the mechanism of diffusion. The first four terms in the right hand side of Eq. (2) are equal to the diffusion coefficient $D(= \gamma l_0^2 v_0 \exp(-\Delta G_m^*/RT))$,¹⁴ and Eq. (2) reduces to the simple form of Eq. (3).⁷

$$\frac{dv}{dt} = D \left(\frac{a_x}{\lambda_x}\right) \left\{1 - \exp\left(-\frac{\Delta G}{RT}\right)\right\} \quad (3)$$

(a_x/λ_x) in Eq. (3) is the term of diffusion area and length for the whole volume V . As volume dv emerging from dV flows from the area $a(x)$ through the mean cross sectional area $a_m(x)$ to the outlet area a_{out} as shown in Fig. 1, (a_x/λ_x) is given by taking a harmonic average of $a_m(x)/\lambda(x)$ over the volume V . $a_m(x)$ is the mean cross sectional area of a truncated cone with bases of $a(x)$ and a_{out} . $\lambda(x)$ is the diffusion length from $a_x(x)$ to a_{out} . $a_m(x)$ is calculated by taking a harmonic average of cross sectional area $a(x)$ from x to x_{out} . (a_x/λ_x) is then given by the following equations.¹¹

$$\frac{1}{a_m(x)} = \frac{\int_{x_{out}}^x \frac{1}{a(x)} dx}{\int_{x_{out}}^x dx}, \quad \text{and} \quad \frac{1}{\left(\frac{a_x}{\lambda_x}\right)} = \frac{\int_V \frac{1}{\left(\frac{a_m(x)}{\lambda(x)}\right)} dV}{\int_V dV} \quad (4)$$

From Eqs. (3) and (4), we can calculate the rate for diffusion material transport activated by excess free energy.

Eq. (3) is valid in a system where a material concentration gradient exists. This is confirmed by derivation of Fick's first law from Eq. (3). In the case of a material where a concentration gradient exists, Eq. (3) is modified to Eq. (5),

$$\frac{dm}{dt} = C_A D \left(\frac{a_x}{\lambda_x}\right) \left\{1 - \exp\left(-\frac{\Delta G}{RT}\right)\right\} \quad (5)$$

where C_A is the concentration of material A and dm is diffusing material. The chemical potential μ_A of material A is:

$$\mu_A = \mu_A^0 + RT \ln a_A = \mu_A^0 + RT \ln f_A C_A \quad (6)$$

where μ_A^0 , a_A , and f_A are the standard chemical potential, the activity and the activity coefficient,¹⁵ respectively. μ_A^0 is a constant, and f_A does not depend on the concentration C_A for an ideal and dilute solution. When the small volume dV has the concentration gradient dC_A/dx , the free energy change ΔG by material flow in the small volume dV is evaluated by Eq. (7).

$$\Delta G (= -d\mu_A) = -\left(\frac{RT}{C_A}\right)dC_A \quad (7)$$

As (a_x/λ_x) is equal to $\{a(x)/dx\}$ in dV , substituting Eq. (7) for ΔG , Eq. (5) becomes Fick's first law as shown by Eq. (8).

$$\begin{aligned} \frac{dm}{dt} &= C_A D \left\{ \frac{a(x)}{dx} \right\} \left\{ 1 - \exp\left(\frac{RTdC_A}{C_A RT}\right) \right\} \\ &\approx -a(x)D \frac{dC_A}{dx} \end{aligned} \quad (8)$$

The free energy theory for material transport is thus coincident with Fick's law. If material flows along concentration gradient, material transport is naturally calculated by Fick's law. On the other hand, the free energy theory can be adopted in the case of material transport driven by surface energy as discussed in the next section.

3. Rate equation for shape change of spheroidal and rectangular grains

3.1. Models and excess energy for shape change of spheroidal and rectangular grains

We consider here simple cases of shape changes occurring in spheroidal and rectangular solid grains. Fig. 2 shows models for two grains which are expressed by Eq. (9).

For spheroidal grains,

$$\frac{x^2}{r_a^2} + \frac{y^2}{r_b^2} + \frac{z^2}{r_b^2} = 1, \text{ and } r_a > r_b > 0.$$

For rectangular grains,

$$x = \pm r_a, y = \pm r_b, z = \pm r_b, \text{ and } r_a > r_b > 0. \quad (9)$$

The spheroidal grain has an ellipsoidal surface of revolution, and the rectangular grain has a parallelepiped shape with two square bases. Both grains are symmetric around the x-axis and elongated in the x direction. They are not in an equilibrium state. If diffusion is activated enough, they will gradually change their shapes to equilibrium shapes keeping symmetry around x-axis. The equilibrium shapes of spheroid and rectangular grains are obviously a sphere and a cube, respectively.

The surface energy of grain at the present (non-equilibrium) state $\phi(\text{at present})$ is calculated by Eq. (10) in units of J/mole using parameters of surface energy ϵ_s , surface area S , grain volume V , and molar volume of solid V_m .

$$\phi(\text{at present}) = \frac{\epsilon_s S}{(V/V_m)} \quad (10)$$

Excess free energy is given by the difference between $\phi(\text{at present})$ and minimum surface energy $\phi(\text{at equilibrium})$.

$$\Delta G = \phi(\text{at present}) - \phi(\text{at equilibrium}) \quad (11)$$

The surface areas and volumes of spheroidal and rectangular grains are $2\pi\left[r_b^2 + \left\{r_a^2 r_b / (r_a^2 - r_b^2)\right\}^{1/2} \text{Arccos}(r_b/r_a)\right]$ and $4\pi r_a r_b^2/3$, and $16r_a r_b + 8r_a^2$ and $8r_a r_b^2$, respectively. At equilibrium, r_a is equal to r_b , and ΔG is calculated by the following equations.

For spheroidal grains

$$\Delta G = \left(\frac{\epsilon_s V_m}{r_a}\right) 3R_a^{-2/3} \left[\frac{1}{2} R_a^{2/3} \left\{ 1 + \frac{\text{Arccos} R_a}{R_a (1 - R_a^2)^{1/2}} \right\} - 1 \right].$$

For rectangular grains

$$\Delta G = \left(\frac{\epsilon_s V_m}{r_a}\right) 3R_a^{-2/3} \left\{ \frac{1}{3} R_a^{-1/3} (2 + R_a) - 1 \right\}. \quad (12)$$

where $R_a = r_b/r_a$ ($0 < R_a \leq 1$) is the shape factor. For $R_a < 1$, grains are elongated, and they become a sphere or a cube at $R_a = 1$.

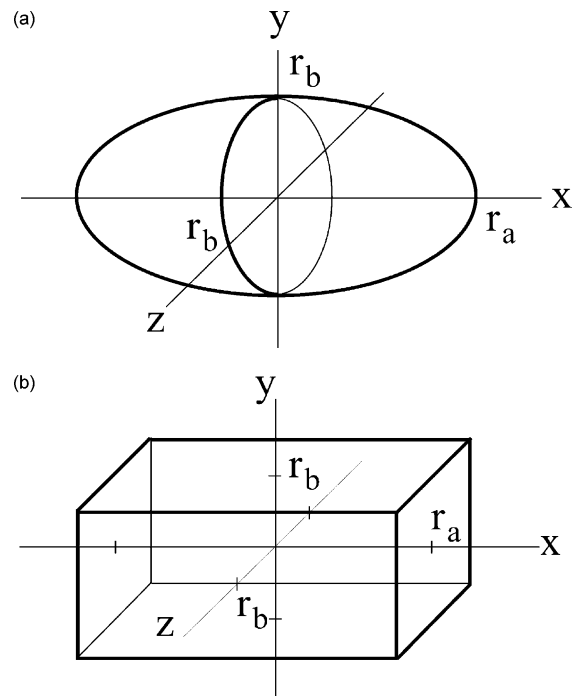


Fig. 2. Models for (a) spheroidal grain and (b) rectangular grain. Both grains are symmetric around the x-axis and elongate in the x direction.

3.2. Term of diffusion area and length

While spheroidal and rectangular grains deform toward equilibrium shapes, material transport by diffusion takes place in the grains. Although the exact diffusion path is not known, we can, however, consider that the diffusion path is approximately the same path through which material flows into a central plane from the whole volume. Fig. 3 shows that volume dv flows from volume dV_1 in V_1 into the plane a_{out} . Calculation of (a_x/λ_x) is therefore performed on V_1 and V_2 using Eq. (13).

$$\frac{1}{\left(\frac{a_x}{\lambda_x}\right)} = \frac{\int_{v_1} \frac{1}{\frac{a_m(x)}{\lambda(x)}} dV + \int_{v_2} \frac{1}{\frac{a_m(x)}{\lambda(x)}} dV}{\int_V dV} \quad (13)$$

$a_m(x)$ for spheroidal and rectangular grains is $\{a(x)a_{out}\}^{1/2} = \pi r_b^2(1-x^2/r_a^2)^{1/2}$ and $4r_b^2$, respectively, and $\lambda_x = |x|$. By carrying out the integral in Eq. (13), we get the term of diffusion area and length (a_x/λ_x) .

For spheroidal grains

$$\left(\frac{a_x}{\lambda_x}\right) = 2\pi r_a R_a^2.$$

For rectangular grains

$$\left(\frac{a_x}{\lambda_x}\right) = 8r_a R_a^2. \quad (14)$$

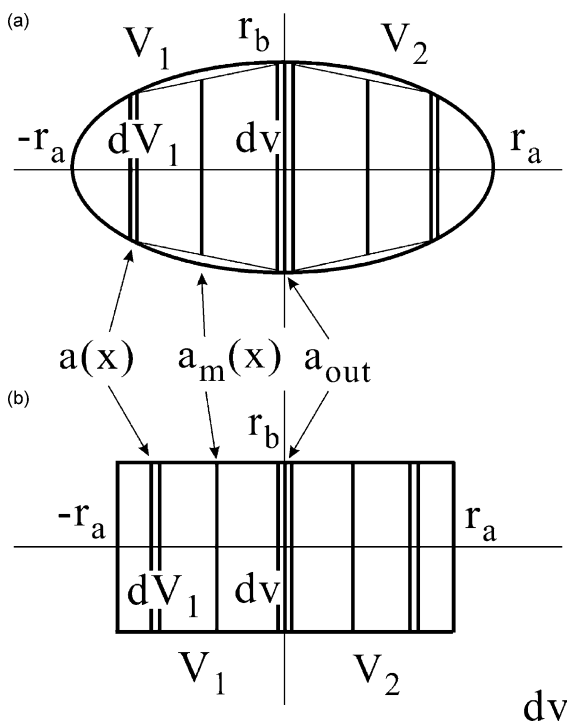


Fig. 3. Volume dv diffusing in (a) spheroidal grain and (b) rectangular grain. dv flows from small volume dV_1 with cross-sectional area $a(x)$ through mean cross-sectional area $a_m(x)$ to outlet a_{out} . The same volume dv also flows from V_2 .

3.3. Rate equations for shape change of grains

In the same way as the calculation of the term of diffusion area and length, the volume required for a shape change of a grain is considered to be equal to $2dr_a \times a_{out}$. Thus dv/dt is:

For spheroidal grains

$$\frac{dv}{dt} = \frac{4\pi}{3} r_a^3 R_a \frac{dR_a}{dt}.$$

For rectangular grains

$$\frac{dv}{dt} = \frac{16}{3} r_a^3 R_a \frac{dR_a}{dt}. \quad (15)$$

From Eqs. (3), (12), (14) and (15), we obtain the rate equations for shape changes of spheroidal and rectangular grains.

For spheroidal grains

$$\frac{dR_a}{dt} = \left(\frac{3\varepsilon_s D V_m}{RT}\right) \frac{1}{V} \cdot 2\pi R_a^{7/3} \left[\frac{1}{2} R_a^{2/3} \left\{ 1 + \frac{\text{Arccos} R_a}{R_a(1-R_a)^{1/2}} \right\} - 1 \right].$$

For rectangular grains

$$\frac{dR_a}{dt} = \left(\frac{3\varepsilon_s D V_m}{RT}\right) \frac{1}{V} \cdot 12 R_a^{7/3} \left\{ \frac{1}{3} R_a^{-1/3} (2 + R_a) - 1 \right\}. \quad (16)$$

ε_s , D and V_m are material constants, and the volume V is the same in both grains. The rates of shape change are in proportion to the surface energy ε_s and the diffusion constant D and in inverse proportion to the volume V .

4. Behavior of shape changes of spheroidal and rectangular grains

4.1. Calculation of rates for shape change

The rates for shape change dR_a/dt were calculated using Eq. (16). The results are shown in Fig. 4, where dR_a/dt is normalized by the factor $B = (3\varepsilon_s D V_m / RT) / V$ and plotted against R_a . The calculations were performed from $R_a = 0.5-1$. A small value of $R_a < 0.5$ is not adequate for the models in Fig. 2, because spheroidal and rectangular grains get too long and narrow. In such narrow grains, the approximation for the term of diffusion area and length adopted in Section 3.2 may not be adequate. Fig. 4 indicates that dR_a/dt becomes larger as R_a becomes smaller, that is, a long and narrow grain

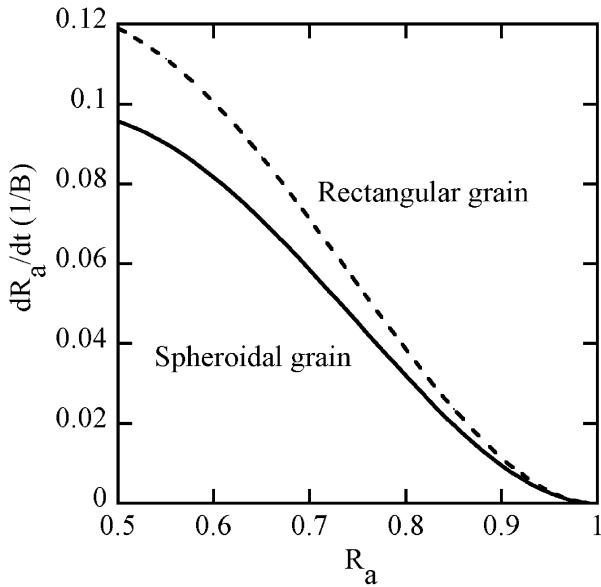


Fig. 4. Rate of shape change dR_a/dt for spheroidal grain and rectangular grain as a function of grain shape factor R_a , where $B = (3\varepsilon_s DV_m/RT)/V$.

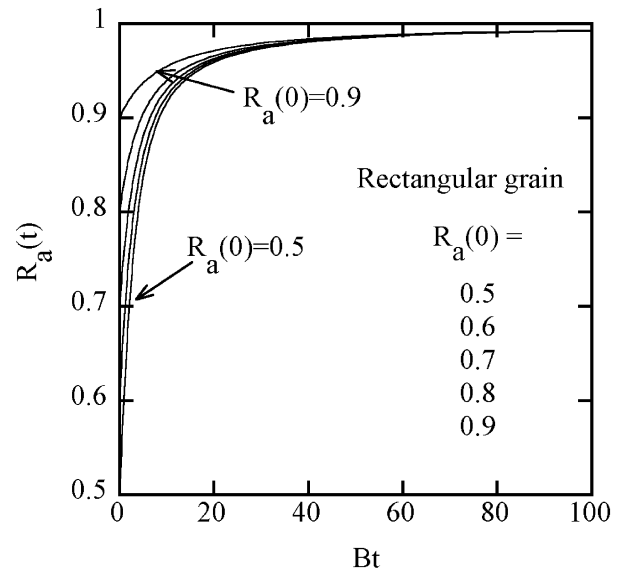


Fig. 6. Shape change of rectangular grain. Shape factor at time t $R_a(t)$ is plotted against non dimensional time Bt , where B is $(3\varepsilon_s DV_m/RT)/V$. The calculations were performed varying initial grain shape factors $R_a(0)$, $R_a(0) = 0.5, 0.6, 0.7, 0.8$ and 0.9 .

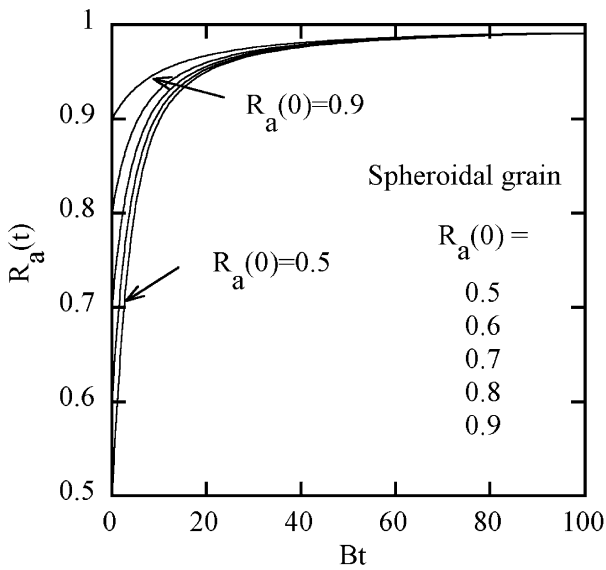


Fig. 5. Shape change of spheroidal grain. Shape factor at time t $R_a(t)$ is plotted against non dimensional time Bt , where B is $(3\varepsilon_s DV_m/RT)/V$. The calculations were performed with changing initial grain shape factor $R_a(0)$, $R_a(0) = 0.5, 0.6, 0.7, 0.8$ and 0.9 .

rapidly changes its shapes. The figure also shows that dR_a/dt for a rectangular grain is always larger than that for a spherical grain.

4.2. Behavior of shape change of spheroidal and rectangular grains

Behavior of shape change was simulated using Eq. (16). Given that grain had a shape factor $R_a(t)$ at time t , $R(t+dt)$ after a small range of time dt was obtained by

adding $dt \times dR_a(t)/dt$ to $R_a(t)$. The calculations were repeated varying the initial shape factor $R_a(0)$ from 0.5 to 0.9. Figs. 5 and 6 show $R_a(t)$ as a function of the normalized time Bt . The shape factor $R_a(t)$ for all $R_a(0)$ increased rapidly from $Bt=0$ to $Bt \approx 10$, and then it increased very slowly toward $R_a(t)=1$ where the spheroidal and the rectangular grains are nearly a sphere and a cube, respectively. It was found that elongated grains changed their shapes very rapidly, while nearly round and cubic grains changed shapes very slowly.

Comparing carefully the shape factor $R_a(t)$ in Figs. 5 and 6, it is noticed that the rectangular grain changes its shape a little faster than the spheroidal grain. This is in accordance with the result that dR_a/dt is always larger for the rectangular grain than for the spheroidal grain as shown in Fig. 4. This behavior can be understood by considering that the surface area of a spheroidal grain is smaller than that of a rectangular grain with the same volume V .

It may be interesting to estimate the actual grain size which may show rapid shape change. For this estimation, we can utilize the diffusion coefficient and surface energy data of, for instance, SiC ceramics reported in the literature.^{16–18} SiC fine powder is usually sintered at about 2000–2200 °C.^{19–22} Diffusion in SiC solid is activated at that temperature, so that we assume that SiC grain may actually change its shape by heating at 2000 °C for about 1 h (= Δt). This time corresponds 10 for Bt in Figs. 5 and 6, where $R_a(t)$ rapidly decreases. The lower diffusion species in SiC is Si, and its lattice diffusion coefficient D is about 4.9×10^{-18} m²/s at 2000 °C for a pure single crystal.¹⁶ Surface energy ε_s is estimated to be about 3.5 J/m²,¹⁸ and molar volume V_m

is $1.25 \times 10^{-5} \text{ m}^3/\text{mole}$.²³ From $Bt = (3\varepsilon_s D V_m / RT)(1/V)\Delta t$ using the values of ε_s , D , V_m , Dt and Bt , the volume V is calculated as $1.2 \times 10^{-23} \text{ m}^3$ and r_a for spherical grain is 14 nm. We can speculate from this result that SiC grain will change its shape toward an equilibrium shape at 2000 °C if its grain size is in the order of several tens of nm.

In this work we considered shape change of grains only by the lattice diffusion mechanism. Shape change can also take place by surface diffusion, vaporization and condensation. For these mechanisms, (a_x/λ_x) in Eq. (14) and dv/dt in Eq. (15) must be re-calculated. It is not, however, possible to calculate eq.14 by the usual analytical method. We need some numerical simulation, which will be performed by further work.

The estimated grain radius of 14 nm mentioned above seems to be a little smaller than expected, because SiC powder actually sintered if grains are sub-micron size ($> \sim 0.5 \mu\text{m}$). This may be due to using a lower lattice diffusion coefficient and ignoring surface diffusion mechanism. The diffusion coefficient used for the calculation was that of a large pure SiC crystal. The actual diffusion coefficient for small SiC grain may be larger because it is not pure and contains many defects and contaminations. Both increase the diffusion coefficient very much. Surface diffusion also transports material very much faster than the lattice diffusion. We should consider these factors for exact calculation of shape changes of grains.

5. Conclusions

The free energy theory for material transport of solids was first discussed in this article. The theory assumed that material transport in a system was activated in proportion to the total amount of excess free energy so that the system became an equilibrium state. From the theory, the rate equation for diffusion material transport was derived. The material transport rate was given by the products of the diffusion coefficient, the terms of diffusion area and length, and the term of activation energy.

Second, shape changes occurring in spheroidal and rectangular grains were theoretically investigated based on the theory. Excess surface energy was assumed to drive shape changes of spheroidal and rectangular grains toward equilibrium shapes of a sphere and a cube, respectively. From this assumption the rate equations for shape changes were obtained. The shape changes were then simulated by calculations of the shape factor. It was found that elongated grains changed their shapes rapidly, while nearly round and cubic grains changed shapes very slowly.

References

1. Reed, J. S., Ceramic raw materials. In *Principles of Ceramics Processing*. John Wiley & Sons, New York, 1995, pp. 33–66.
2. Konishi, M., Noguchi, H. and Kijima, K., Preparation of ultra-fine SiC powders by plasma CVD and sintering. In *Silicon Carbide Ceramics-2*, ed. K. Somya and S. Inomata. Elsevier Applied Science, London and New York, 1991, pp. 61–79.
3. Kingery, W. D., Bowen, H. K. and Uhlmann, D. R., Grain growth, sintering and vitrification. In *Introduction to Ceramics*. John Wiley & Sons, New York, 1976, pp. 448–515.
4. German, R. M., Solid state sintering fundamentals. In *Sintering Theory and Practice*. John Wiley & Sons, New York, 1996, pp. 67–141.
5. Pan, J., Le, H., Kucherenko, S. and Yeomans, J. A., A model for the sintering of spherical particles of different sizes by solid state diffusion. *Acta Mater.*, 1998, **46**, 4671–4690.
6. Fischmeister, H. and Grimvall, G., Ostwald ripening—a survey. In *Sintering and Related Phenomena*, ed. G. C. Kuczynski. Plenum Press, New York, 1973, pp. 119–149.
7. Inomata, Y., Free energy theory of the initial sintering of solids. *J. Ceram. Soc. Japan*, 1982, **90**, 527–531.
8. Inomata, Y., Free energy theory of material transport for sintering and diffusional creep. In *Proceedings of First International Symposium on Ceramic Components for Engine*, ed. S. Somya, E. Kanai and K. Ando. Reidel Publishing Co, Dordrecht-Boston-Lancaster, 1984, pp. 753–761.
9. Inomata, Y., Free energy theory of material transport controlled by diffusion. *J. Surface Sci. Soc. Japan*, 1984, **5**, 308–312.
10. Tanaka, H., Sintering and grain growth rates of two spheres with different Radii. *J. Ceram. Soc. Japan, Int. Ed.*, 1995, **103**, 138–143.
11. Tanaka, H., Normal and abnormal grain growth rate in a spherical grain matrix. *J. Ceram. Soc. Japan*, 1996, **104**, 253–258.
12. Tanaka, H., Rate equations for sintering and grain growth with two-sphere model, theory of grain coalescence. In *The Science of Engineering Ceramics II, Key Engineering Materials Vols. 161–163*, ed. K. Niihara, T. Sekine, E. Yasud and T. Sasa. Trans Tech Publications Ltd, Zurich Switzerland, 1999, pp. 457–460.
13. Inomata, Y., Rate process in brittle fracture. *J. Surface Sci. Soc. Japan*, 1989, **10**, 187–194.
14. Shewmon, P. G., Atomic theory of diffusion. In *Diffusion in Solids*. McGraw-Hill, New York, 1963, pp. 40–85.
15. DeHoff, R. T., Multicomponent, homogeneous nonreacting system: solutions. In *Thermodynamics in Materials Science*. McGraw-Hill, New York, 1993, pp.160–207.
16. Hong, J. D., Hon, M. H. and Davis, R. F., Self-diffusion in alpha and beta silicon carbide. *Ceramurgia Int.*, 1979, **5**, 155–160.
17. Bruce, R. H., Aspects of the surface energy of ceramics I—calculation of surface free energies. In *Science of Ceramics Vol. 2*, ed. G. H. Stewart. Academic Press, London, 1965, pp. 359–381.
18. Inomata, Y. and Matsumoto, S., On the formation of β -SiC in the initial growth stage. *J. Ceram. Soc. Japan*, 1971, **79**, 40–46.
19. Prochazka, S., The role of boron and carbon in the sintering of silicon carbide. In *Special Ceramics 6*, ed. P. Popper. The British Ceramics Research Association, Stoke-on-Trent, 1975, pp. 171–181.
20. Böker, W. and Hausner, H., The influence of boron and carbon additions on the microstructure of sintered alpha silicon carbide. *Powder Metall. Int.*, 1978, **10**, 87–89.
21. Dudda, S., Densification and properties of α -silicon carbide. *J. Am. Ceram. Soc.*, 1985, **68**, C269–C270.
22. Tanaka, H. and Iyi, N., Polytype, grain growth, and fracture toughness of metal boride particulate SiC composites. *J. Am. Ceram. Soc.*, 1995, **78**, 1223–1229.
23. Powder diffraction file JCPDS 29-1128 compiled by the ICDD. International center for diffraction data, Newton square (PA), 1979.